RESEARCH ARTICLE

Unveiling the potential antibacterial mechanism of *Melaleuca cajuputi* leaf extract by cell morphology studies and molecular docking analysis

Musa Isah[1,2] · Wan-Nor-Amilah Wan Abdul Wahab[2] · Hasmah Abdullah[2] · Shajarahtunnur Jamil[3] · Mohd Dasuki Sul'ain[2] · Abdullahi Ibrahim Uba[4] · Gokhan Zengin[5] · Dibyajit Lahiri[6] · Hisham Atan Edinur[7] · Wan Rosli Wan Ishak[2]

Abstract

The antimicrobial properties of the *Melaleuca cajuputi* plant have been documented. However, the underlying antimicrobial mechanisms remain relatively unexplored. Thus, this study aimed to investigate the antibacterial effects of *M. cajuputi* leaf extract against selected bacterial strains and unveil the potential antibacterial mechanisms of the most potent sub-fraction through time-kill assay, cell morphology studies, and molecular docking analysis. The fractions and sub-fractions were obtained from the methanolic extract of *M. cajuputi* leaf by bioassay-guided fractionation. The antibacterial activity was tested against *Staphylococcus aureus, Streptococcus agalactiae, Klebsiella pneumoniae,* and *Escherichia coli* using broth microdilution assay. The most potent sub-fraction, Melaleuca fraction 2d (MF2d), demonstrated remarkable antibacterial activity with MIC values ranging from 0.063 to 0.25 mg/mL and induced significant cellular damage against the tested bacteria. The chemical characterization of the most potent sub-fraction (MF2d) from methanolic extract of *M. cajuputi* leaf identified five (5) compounds with 2-isopropyl-10-methyl phenanthrene (83.09%) as the major component. *In-silico* molecular docking analysis revealed that all the docked ligands showed strong binding propensity towards target bacterial proteins, including DNA gyrase (PDB ID: 1ZI0), dihydropteroate synthase (PDB ID: 1AD1), and D-alanyl transferase (PDB ID: 6O93) with the binding energy ranging from − 6.0 to − 8.4 kcal/mol. The overall findings demonstrated the potential of the *M. cajuputi* plant as a valuable source of novel antibacterial agents.

Keywords Antibacterial effects · Chemical characterization · Molecular docking · *Melaleuca cajuputi* · Scanning electron microscopy

✉ Mohd Dasuki Sul'ain
drdasuki@usm.my

Shajarahtunnur Jamil
shajarah@utm.my

Abdullahi Ibrahim Uba
abdullahi.iu2@gmail.com

Gokhan Zengin
gokhanzengin@selcuk.edu.tr

1   Department of Microbiology, Kebbi State University of Science and Technology, P.M.B. 1144, Aliero, Kebbi State, Nigeria

2   School of Health Sciences, Universiti Sains Malaysia, Health Campus, Kubang Kerian, 16150 Kota Bharu, Kelantan, Malaysia

3   Department of Chemistry, Faculty of Science, Universiti Teknologi Malaysia, 81310 Johor Bahru, Johor, Malaysia

4   Department of Molecular Biology and Genetics, Istanbul AREL University, 34537 Istanbul, Turkey

5   Physiology and Biochemistry Laboratory, Department of Biology, Science Faculty, Selcuk University, Konya, Turkey

6   Institute of Engineering and Management, Kolkata University of Engineering and Management, Kolkata, India

7   Forensic Programme, School of Health Sciences, Universiti Sains Malaysia, Health Campus, Kubang Kerian, 16150 Kelantan, Malaysia

Introduction

Infectious diseases caused by microorganisms are a leading cause of death and morbidity in humans globally (Manandhar et al. 2019). Although various antibiotics have been developed to tackle these diseases with maximum efficacy, their irrational use and microbial evolution have resulted in drug-resistant strains (Abushaheen et al. 2020). The increasing prevalence of drug resistance, the adverse effects of synthetic antibiotics, and the reemergence of diseases have necessitated searching for novel therapeutic agents from natural resources such as medicinal plants (Manga et al. 2017; Shubham et al. 2018). Medicinal plants have played an essential role in primary health care and are a valuable source of novel bioactive compounds for drug development (Anza et al. 2021). The pharmacological properties of plants could be attributed to their enormous bioactive compounds, including essential oils, alkaloids, flavonoids, tannins, phenolic acids, and terpenoids (Anza et al. 2021; Gorlenko et al. 2020; Mera et al. 2019).

Melaleuca cajuputi, also known as Gelam in Malaysia or Cajuput tree in English, has been traditionally used in folk medicine to treat respiratory and urinary tract infections and muscle and joint pain (Isah et al. 2022). This plant belongs to the Myrtaceae family and has documented pharmacological properties (Bua et al. 2020; Septiana et al. 2020; Toan et al. 2020). The plant collection includes over 200 species, mainly native to Australia, with a few also found in Southeast Asia and nearby islands (Awam 2023). Several studies have reported the antimicrobial activities of *M. cajuputi* leaf crude extracts and essential oils (Bua et al. 2020; Isnaini et al. 2021; My et al. 2020; Wan-Nor-Amilah et al. 2022). However, the underlying antimicrobial mechanisms are relatively unexplored. Hence, this study aimed to investigate the antibacterial effects of *M. cajuputi* leaf extract and examine the potential antibacterial mechanisms of the most potent sub-fraction by time-kill assay, cell morphology studies and in silico molecular docking analysis.

Material and methods

Plant material collection and extract preparation

Melaleuca cajuputi leaves were collected from Bachok, Kelantan, Malaysia, and authenticated by a botany expert at the International Islamic University Malaysia (IIUM). The voucher specimen number (PIIUM 0304) was deposited at the University Herbarium unit for reference. The leaf samples were cleaned extensively in flowing tap water to eliminate soil particles and attached debris and then rinsed with sterile distilled water. The leaves were cut, shade-dried, and pulverized into a fine powder using a mechanical grinder (SY-10 ID446524). The extraction process was carried out as described by Al-Abd et al. (2015) and Khalaf et al. (2021). Two hundred (200 g) pulverized leaf samples were macerated in 2 L of methanol (1:10 w/v). The extraction was carried out for 72 h at room temperature, with intermittent stirring. The extracts were filtered with Whatman No. 1 filter paper and concentrated to dryness using a rotary evaporator (Hei-VAP, Germany) at 50 °C and reduced pressure. The residual solvent was evaporated in hot air oven at 35 °C. The extracts were then freeze-dried using a freeze-dryer (ilShin Lab Co., Ltd. Korea) at − 50 °C under a vacuum yielding dry residue. The dried methanolic extract was stored at 4 °C until needed for further analysis.

Solvent selection for the fractionation of the crude extract

Thin-layer chromatography (TLC) was performed to determine the optimal solvent system for fractionating the extract using vacuum liquid chromatography (VLC). Five hundred (500 μg/mL) of the crude extract were prepared using methanol and applied onto TLC micro slides of the aluminium sheath (2 × 10 cm) pre-coated with silica gel 60_{F254} (Merck). Plate marking was done using a soft pencil, with a single dot per slide. Glass capillaries were used to spot the sample onto the TLC plate. The extract on the slides was separated using different solvent systems with varying polarities, ranging from non-polar to highly polar solvents until the best solvent system was obtained, which was hexane, ethyl acetate, and methanol at a ratio of 85:10:5. This solvent system was used for the subsequent bioassay-guided fractionation.

Bioassay-guided fractionation

Ten (10 g) of the methanolic extract was fractionated using vacuum liquid chromatography (VLC) on silica gel 60 (0.040–0.063 mm) (230 g) as a stationary phase. The column was sequentially eluted using the solvent system obtained from plate TLC: hexane, ethyl acetate (EtOAc), and methanol (MeOH). A volume of 100 mL of hexane was initially used, followed by the addition of 10% EtOAc, resulting in a ratio of 90:10 v/v. The volume of EtOAc was increased by 10% to a maximum of 100%, leading to a gradual shift in the polarity of the solvent system from 100% hexane. The solvent system was subsequently changed to a combination of EtOAc and MeOH, with an initial ratio of 10% MeOH and 90% EtOAc. This solvent system was gradually adjusted to 100% MeOH and yielded twenty-two fractions.

Fractions with comparable TLC profiles were merged to obtain the Melaleuca fraction (MF), viz MF1, MF2, MF3, and MF4. All these fractions were evaluated against four bacterial strains, and the most potent fraction based on the MIC values was selected for further fractionation using column chromatography.

The most potent fraction was eluted on silica gel 60 (0.063–0.200 mm) using column chromatography for further separation of the bioactive compounds. Hexane and EtOAc were used as the solvent system in increasing order of polarity (100:0, 99:1, 98:2, and 97:3 v/v) and yielded 140 fractions. Aliquots (5 µL) of the 140 fractions from the most potent fraction were spotted on TLC slides of the aluminium sheath (L×W 5×4 cm) pre-coated with silica gel 60_{F254} (Merck). The spotted plates were developed in hexane and EtOAc as mobile phase at 25 °C. The plates were dried and visualized under UV light at 254 and 360 nm, then sprayed with 5% sulfuric acid in vanillin reagent and heated at 100 °C for 5 min. Fractions with similar TLC profiles were pooled into four sub-fractions, namely MF2a, MF2b, MF2c, and MF2d. These sub-fractions were also concentrated and tested for antibacterial activity (Erhabor et al. 2021; Mroczek et al. 2020).

Antibacterial assays

Test bacteria and inoculum preparation

The bacterial strains used in this study were obtained from the Microbiology laboratory at the School of Health Sciences, Universiti Sains Malaysia. The bacterial strains include *Staphylococcus aureus* ATCC 25923, *Streptococcus agalactiae* ATCC 13813, *Klebsiella pneumoniae* ATCC 1706, and *Escherichia coli* ATCC 25922. A standardized inoculum was prepared by selecting bacterial colonies with similar characteristics from a fresh agar plate culture and inoculated into Mueller Hinton broth (MHB). Using the optical density measurement at 620 nm, the bacterial suspension was adjusted to the 0.5 McFarland turbidity standard (10^8 CFU/mL).

Broth microdilution assay

The fractions and sub-fractions obtained from the methanolic extract were reconstituted in 2% dimethyl sulfoxide (DMSO) and serially diluted from 1 to 0.015 mg/mL in cation-adjusted Mueller–Hinton broth (MHB) in a 96-well microplate. The standardized bacterial suspension was used to prepare the working suspension, and 100 µL was inoculated into each well. The extract-free solution was used as a blank, while 2% DMSO was used as the negative control. The plates were incubated at 37 °C for 18 h. After incubation, 40 µL of p-iodonitrotetrazolium violet solution (0.2 mg/mL) was used as an indicator of bacterial growth.

The plates were then incubated for the second time at 37 °C for 1 h. Inhibition of bacterial growth is observed when the solution in the well remains clear after incubation with INT. Bacterial growth (no inhibition) results in a red-pink formazan formation in the wells. Meanwhile, the concentration that suppresses bacterial growth and inhibits the formation of a red-pink color was considered the MIC. The MBC values were determined by transferring 10 µL of the culture from the wells that showed growth inhibition from the MIC assay onto the Mueller–Hinton agar (MHA) plates. The plates were then incubated at 37 °C for 18 h. The MBC values were determined as the concentrations that kill 99.99% of the bacteria cells (Al-Abd et al. 2015; Erhabor et al. 2021). The sub-fraction with the highest antibacterial activity was selected for further analysis.

Spectroscopic analysis using FTIR

The most potent sub-fraction was analyzed using the Perkin Elmer FTIR Spectrometer Frontier to determine the functional groups of the bioactive compounds. Potassium bromide (KBr) powder was combined with a sample weighing 10 mg to form a thin pellet called a KBr disc to analyze the functional groups in the most potent sub-fraction. The samples were scanned in the mid-infrared regions (4000 cm^{-1} to 400 cm^{-1}). The infrared absorption bands were interpreted by referencing a standard table of infrared spectra (Nandiyanto et al. 2019; Paosen et al. 2017).

Chemical composition determination using GC–MS

The GC–MS analysis was conducted using the method of Toan et al. (2020). with minor adjustments. The chemical composition of the most potent sub-fraction was identified using (GC–MS Agilent 7890A/5975C GC–MS system, which was linked with an ISQ7000 mass spectrometer system, coupled with TG-5MS fused silica capillary column with dimensions of 30 m 0.25 mm i.d and a film thickness of 0.25 µm. Ten (10 mg) of the dry sample was diluted in 1 mL of MeOH, and 1 µL of the sample was injected with a split ratio of 10:1. Helium (99.99%) was used as the carrier gas at a constant flow rate of 1 mL/min, and the oven temperature was programmed. A full-scan mass spectrum was obtained over the 40–500 m/z scan range, and a total ion chromatogram (TIC) was generated. The MS was measured at several points on each GC peak to ensure its purity. All compounds were tentatively identified using a mass spectral database search (National Institute of Standards and Technology (NIST), which was then compared to the obtained MS data to evaluate the degree of match.

Time-kill assay

The antibacterial action of the most potent sub-fraction towards selected bacterial strains was evaluated using the time-kill assay (Chen et al. 2018). The sample was dissolved in 2% DMSO and diluted in MHB at $1 \times$ MIC, $2 \times$ MIC, and $4 \times$ MIC. An OD of 5×10^5 CFU/mL bacterial inoculum (*S. aureus* and *K. pneumoniae* as representative of Gram-positive and Gram-negative bacteria, respectively) was added to each tube containing MHB and test samples. The negative control (growth control) was prepared by combining a bacterial inoculum with a 2% DMSO solution in a separate tube. The tubes were incubated in a shaker incubator (Thermo Scientific, 420, USA) at 37 °C and 200 rpm for 0, 2, 4, 8, 12, and 24 h. After incubation, a 1 mL sample was diluted tenfold from each tube, and 100 µL from each dilution was plated on MHA plates and incubated at 37 °C for 24 h. The colonies were counted, and the CFU/mL was determined. The experiment was performed in duplicate thrice.

Scanning *electron* microscopy (SEM)

The cell morphology studies of the most potent sub-fraction against the selected bacterial strains (*S. aureus* and *K. pneumoniae* as representative for Gram-positive and Gram-negative bacteria, respectively) were performed according to the method described by Guimarães et al. (2019). The bacterial cells were treated with 2% DMSO (negative control), $1 \times$ MIC of MF2d, and incubated in a shaker incubator for 12 h (at 200 rpm, 37 °C). The suspensions were centrifuged (4500 rpm, for 10 min, at 4 °C), fixed with McDowell-Trump fixative, and washed twice with 0.1 M of PBS (phosphate buffer). The pellets were treated with a 1% solution of osmic acid for 1 h, followed by two subsequent washes with distilled water. A graded series of acetones (50%, 75%, 95%, and 100%) was used for dehydration. At 10 min intervals, 100% hexamethyldisilazane (HMDS) was added (2 times). Cells were centrifuged for 5 min (4500 rpm, 4 °C) between

these preparation steps. Specimens were gold-coated and examined under SEM (Fei Quanta FEG 450, USA).

Molecular modeling

The crystal protein structures of target bacterial proteins were downloaded from the protein data bank (PDB) (https://www.rcsb.org/). All proteins were prepared using the PlayMolecule server. The 3D ligand structures identified in MF2d were downloaded from the ChEMBL database (https://www.ebi.ac.uk/chembl/) and optimized using UCSF Chimera (Zengin et al. 2022). All prepared proteins and ligands were converted into PDBQT format. Docking was conducted using AutoDock Vina (PyRx) (https://vina.scripps.edu/) (Mir et al. 2022). The target bacterial proteins and grid center used for each protein are given in Table 1. The binding energy of five ligand poses was computed for each ligand against each protein, and the best pose was saved for post-docking analysis. Protein–ligand interactions were visualized using Biovia DS Visualizer v4.5 (BIOVIA in San Diego, CA, USA) (Saqallah et al. 2022).

Results

Antibacterial assay

From the antibacterial activity results, MF2 was the most potent, with MIC values ranging from 0.063 to 0.25 mg/mL compared to MF1, MF3, and MF4. Hence, MF2 was further fractionated into four sub-fractions (MF2a, MF2b, MF2c, MF2d) and tested for antibacterial activity. MF2d was the most potent, with MIC values (0.063 mg/mL to 0.25 mg/mL) similar to MF2, followed by MF2c with MIC values ranging from 0.13 to 0.25 mg/mL. Based on the MBC/MIC ratio, the MF2d showed bactericidal effects as the ratio was ≤ 4. On the other hand, *S. agalactiae* and *S. aureus* were relatively more susceptible to MF2d than *K. pneumoniae* and *E. coli*

Table 1 Target bacterial proteins and the docking grid center for each protein

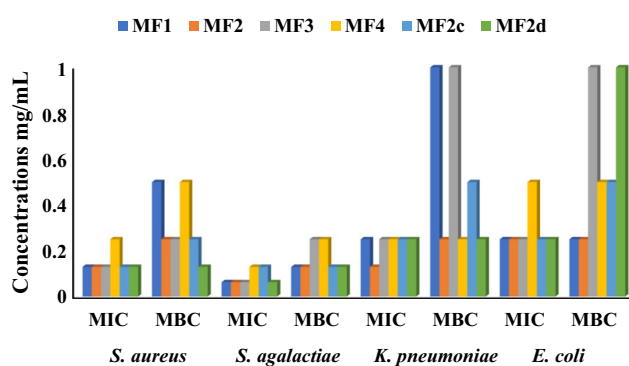| S/no	Target protein /enzyme	PDB ID	Vina grid center		
			X	Y	Z
1	Penicillin-binding proteins (PBPs)	2BG1	30.97	56.41	36.99
2	D-alanyl transferase	6O93	19.45	36.56	51.69
3	DNA gyrase	1ZI0	22.43	34.67	47.23
4	Topoisomerase IV	1S14	− 8.96	− 30.73	10.88
5	Dihydrofolate reductase	1A19	71.2	38.42	22.11
6	Dihydropteroate synthase	1AD1	− 37.55	− 6.49	− 39.02
7	DNA-dependent RNA polymerase	4HDG	34.89	4.11	37.98
8	ABC transporter	3QF4	− 55.05	15.48	40.99

PDB protein data bank

Fig. 1 Antibacterial activity of fractions and sub-fractions obtained from the methanolic extract of *M. cajuputi* leaf. MIC; minimum inhibitory concentration, MBC; minimum bactericidal concentration, MF; Melaleuca fraction

(Fig. 1). MF2a and MF2b showed no activity against all the tested bacterial strains.

Spectroscopic analysis (FTIR)

The functional groups of the bioactive components in MF2d were identified using the FTIR spectrum based on peaks in the Infrared radiation regions within the wavelength range of 4000–400 cm^{-1}. When the sample was run through the FTIR, the functional groups of the components were segregated according to their peak ratios. The FTIR analysis of MF2d revealed the presence of hydrocarbons, amines, aromatics, alcohols, phenol, ethers, and aryl functional groups (Table 2 and Fig. 2).

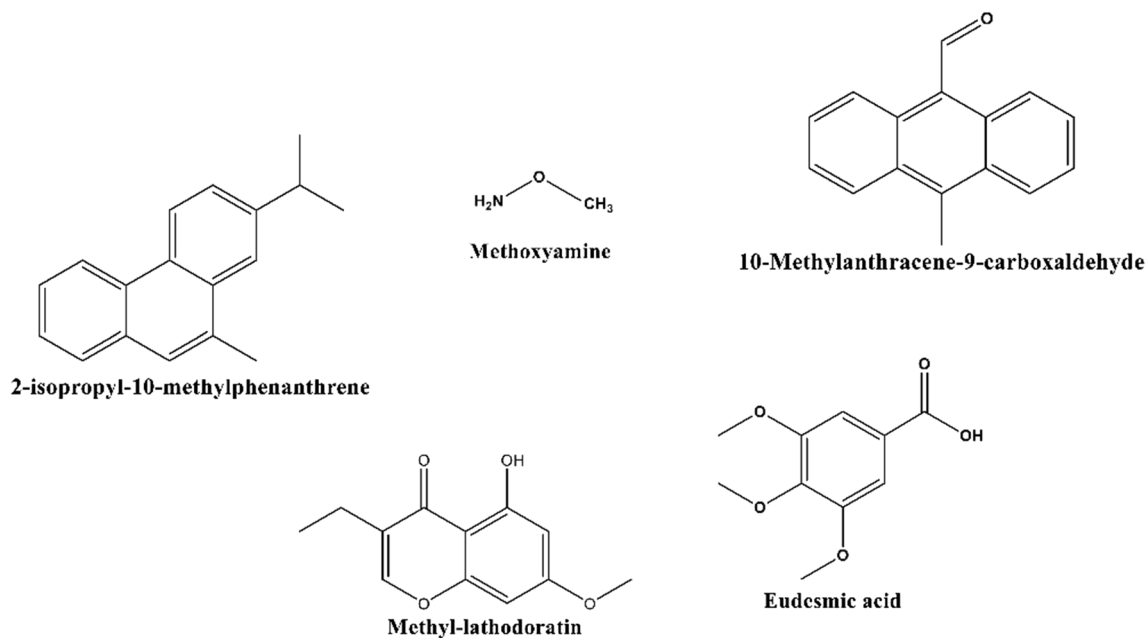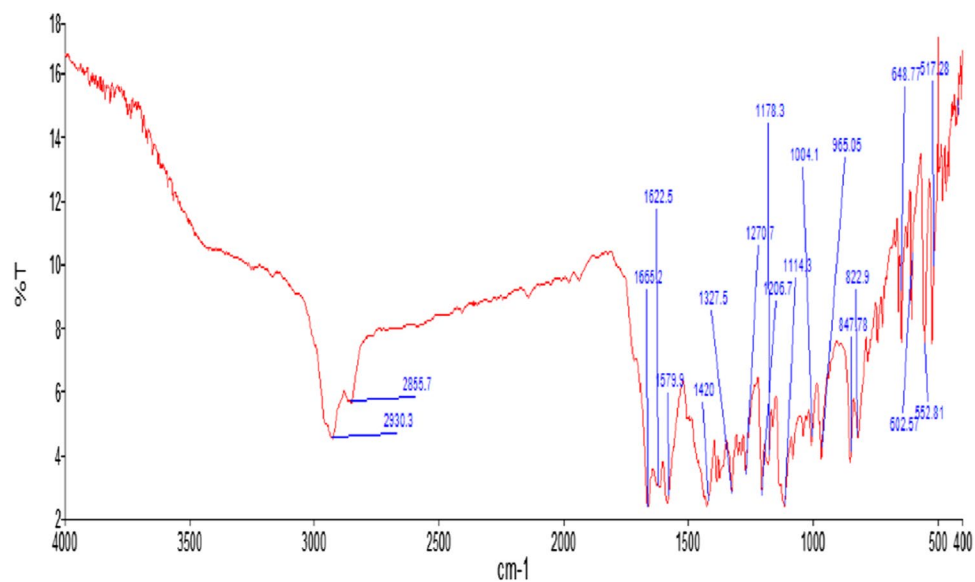## Identification of bioactive components in MF2d by GC–MS

The GC–MS analysis results identified five (5) compounds in MF2d. 2-isopropyl-10-methylphenanthrene (83.09%), 10-methylanthracene-9-carboxaldehyde (10.95%), eudesmic acid (3.58%), d methyl-lathodoratin (2.10%) and methoxyamine (0.28%) Table 4. The chemical structures of the major bioactive components are illustrated in Fig. 3 (Table 3).

Growth curves kinetics

Based on the time-kill assay of MF2d, the bactericidal effect was first observed on *S. aureus* at $2 \times$ MIC after 8h (Fig. 4a) and on *K. pneumoniae* at $2 \times$ MIC after 12 h (Fig. 4b). When the concentration was doubled ($4 \times$ MIC) the bactericidal effect was observed after 4 h against *S. aureus and K. pneumoniae*. The MF2d demonstrated a concentration-dependent impact on the growth of the tested bacteria.

Scanning electron microscopic analysis

The SEM images of 2% DMSO-treated bacteria (control) showed that the DMSO had not caused damage to the treated cells. The bacteria had a spherical and rod-shaped structure, with smooth surfaces and regular clusters (Fig. 5a, c). In contrast, morphological changes characterized by cell shrinkage, cell wall distortion, and abnormal elongation were observed when the bacterial cells were treated with MF2d at $1 \times$ MIC for 12 h (Fig. 5b, d). The effects could be due to cell wall degradation and cellular membrane disruption.

Table 2 FTIR analysis results showing prominent peaks and functional groups in MF2d

S. No	Wavenumber (cm^{-1})	Transmittance (%)	Bond/vibrations	Functional groups
1	2930	4.60	C–H stretch	Alkanes
2	2855	5.73	C–H stretch	Alkanes
3	1665	2.44	C=C stretch	Alkenes
4	1622	3.10	N–H bend	Secondary amine
5	1580	2.87	C=C–C stretch	Aromatics
6	1420	2.65	O–H bend	Alcohols
7	1327	2.86	O–H bend	Phenol
8	1270	3.50	C–O stretch	Aromatic ethers, aryl
9	1206	2.81	C–O stretch	Aromatic ethers, aryl
10	1178	4.09	C–N stretch	Amine
11	1114	2.53	C–N stretch	Amine
12	1004	4.67	C–F stretch	Halo compound
13	965	4.24	C=C bend	Alkene
14	847	4.27	C–Cl stretch	Halo compound
15	822	4.60	C–Cl stretch	Halo compound
16	648–517	8.98	C–Br stretch	Halo compounds

Fig. 2 FTIR spectral profile of MF2d from GC–MS analysis

Fig. 3 Chemical structures of compounds identified in MF2d

Table 3 GC–MS results of MF2d from methanolic extract of *M. cajuputi* leaf

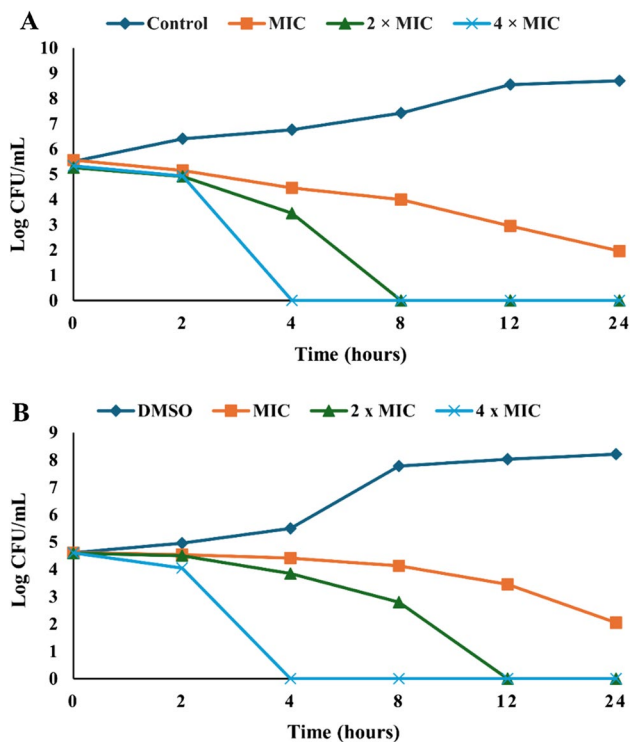| Peak No	Retention time (min.)	Total area %	Molecular formula	Compound name
1	1.277	0.28	CH_5NO	Methoxyamine
2	9.046	3.58	$C_{10}H_{12}O_5$	Eudesmic acid
3	12.249	10.95	$C_{16}H_{12}O$	10-Methylanthracene-9-carboxaldehyde
4	12.466	2.10	$C_{12}H_{12}O_4$	Methyl-lathodoratin
5	12.842	83.09	$C_{18}H_{18}$	2-Isopropyl-10-methyl phenanthrene

Fig. 4 a Time-kill curve for *S. aureus* exposed to 2% DMSO (control) and various concentrations of MF2d at 1×MIC (0.13 mg/mL), 2×MIC (0.26 mg/mL), and 4×MIC (0.52 mg/mL). **b** *K. pneumoniae* exposed to 2% DMSO (control) and various concentrations of MF2d. at 1×MIC (0.25 mg/mL), 2×MIC (0.50 mg/mL), and 4×MIC (1.0 mg/mL)

Molecular docking studies

All ligands (bioactive compounds identified in MF2d) demonstrated potential bindings to the selected bacterial proteins, but a few ligands were predicted to have good binding affinity against some target proteins. For instance, 2-isopropyl-10-methyl phenanthrene demonstrated the highest binding propensity against DNA-dependent RNA polymerase (PDB ID: 4HDG) and moderate binding propensity against D-alanyl transferase (PDB ID: 6O93), DNA gyrase (PDB ID: 1ZI0), and dihydropteroate synthase (PDB ID: 1AD1), with a docked score of − 8.4, − 6.9, − 6.5, and − 6.1 kcal/mol, respectively. Methyl-lathodoratin showed moderate binding to DNA-dependent RNA polymerase, dihydropteroate synthase, and DNA gyrase, with respective docking scores of − 6.8, − 6.2, and − 6 kcal/mol. Meanwhile, 10-methylanthracene-9-carboxaldehyde demonstrated excellent binding to DNA-dependent RNA polymerase and moderate binding to D-alanyl transferase, with respective docking scores of − 7.5 and − 6 kcal/mol (Table 4).

Protein–ligand interaction analysis revealed that 2-isopropyl-10-methyl phenanthrene showed critical interactions with DNA-dependent DNA polymerase, including multiple hydrophobic contacts with leucine (Leu411) and isoleucine (Ile802), while π-sigma and van der Waals interactions reinforced the binding (Fig. 6a). D-alanyl transferase formed a couple of hydrophobic contacts via tryptophan (Trp291) and Ile374, and an H-bond between arginine (Arg276) and the carbonyl oxygen of 10-methylanthracene-9-carboxaldehyde, as well as van der Waals interactions (Fig. 6b). Methyl-lathodoratin occupied the active site of DNA gyrase by forming H-bonds with the backbone of valine (Val737) and the side-chain of Arg739 and Arg838, a π-cation interaction with Arg838, a π-sigma interaction with glutamine (Gln788), a hydrophobic interaction with Ile736, and a few van der Waals interactions (Fig. 6c). The same compound was found in the catalytic cavity of dihydropteroate synthase through H-bonds with threonine (Thr13), Arg52, Val49, and Arg239, as well as a couple of van der Waals interactions all over the channel (Fig. 6d). These ligands-proteins interactions may explain the antibacterial activity of the compounds in MF2d against the bacterial strains.

Discussion

This study examined the antibacterial activity and mechanisms of action of the most potent sub-fraction from *M. cajuputi* leaf extract against selected bacterial strains. The most potent sub-fraction demonstrated remarkable antibacterial activity and caused significant cellular damage against the tested bacteria. The ligand–protein interactions demonstrated a strong binding affinity of the MF2d bioactive compounds towards target bacterial proteins. These findings provide valuable insights into the antibacterial mechanisms of the biologically active compounds in *M. cajuputi* leaf extract and lay the foundation for further investigation of the plant as a novel source of therapeutic agents targeting bacterial infections.

The concentration of plant extracts used for antimicrobial susceptibility testing should be as low as 1 mg/mL, suggesting a strong antimicrobial activity when the MIC value is ≤ 0.1 mg/mL, moderate when the MIC is ≤ 0.625 mg/mL and MIC value > 0.625 mg/mL is considered weak (Mogana et al. 2020). Therefore, MF2d demonstrated moderate to strong antibacterial activity against the tested bacteria, with MIC values ranging from 0.063 to 0.25 mg/mL. Amongst all the sub-fractions, MF2d recorded the lowest MIC values range compared to other sub-fractions. Meanwhile, the MBC values of the MF2d ranged from 0.13 to 1.0 mg/mL. On the other hand, *S. agalactiae* was the most susceptible, followed by *S. aureus, K. pneumoniae*, and *E. coli*. A previous study by Al-Abd et al. (2015) on the antibacterial activity of *M. cajuputi* leaves and flower extracts against eight bacterial strains reported MIC values ranging from 12.5 mg/mL to 25 mg/mL. However, only *S. aureus, Bacillus cereus,* and
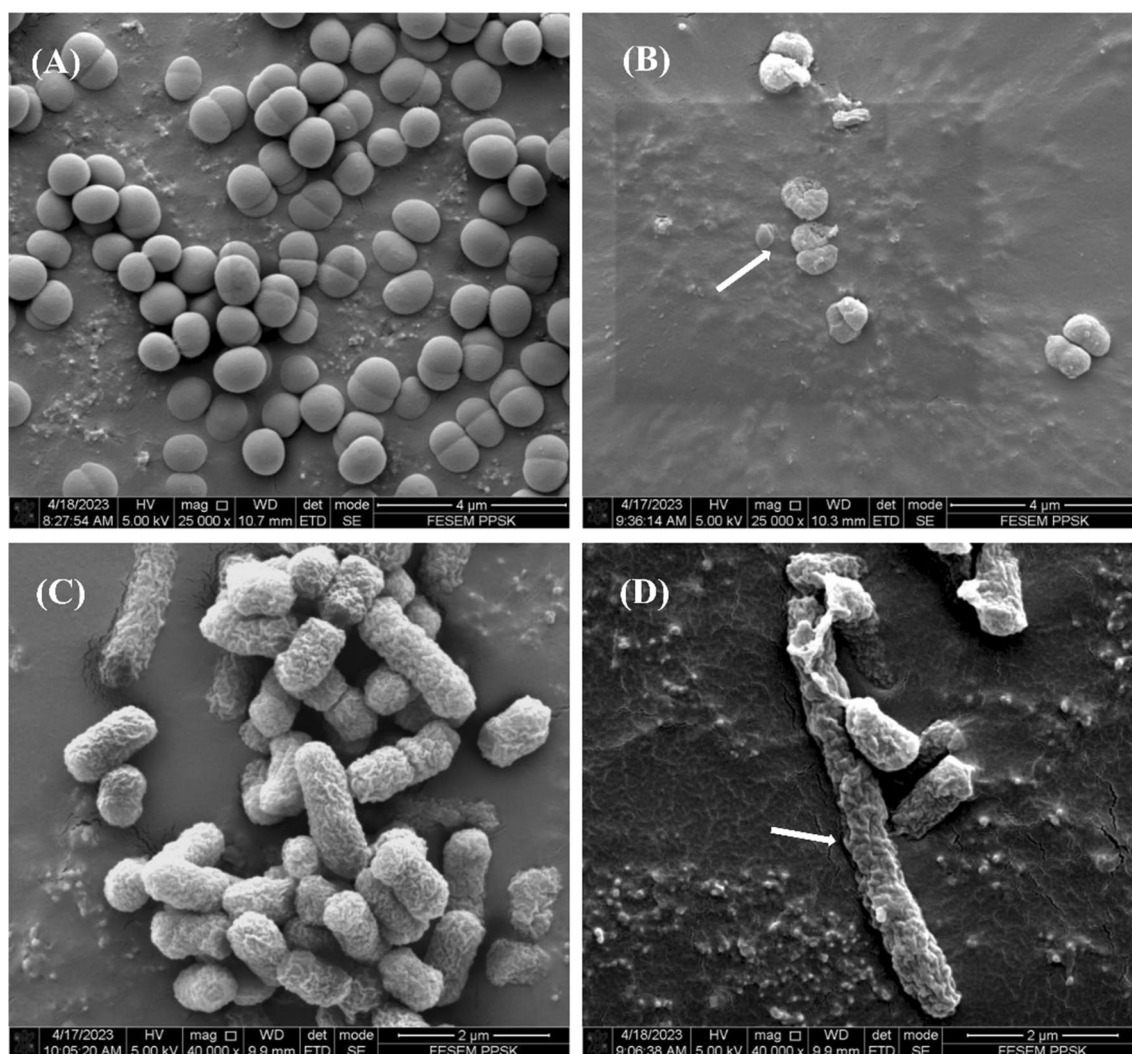
Fig. 5 SEM images of *S. aureus* cells **a)** 2% DMSO-treated cells (control) and **b)** cells treated with 1×MIC (0.13 mg/mL) MF2d **c)** 2% DMSO-treated *K. pneumoniae* cells (control), and **d)** cells treated with 1×MIC (0.25 mg/mL) MF2d. Arrows indicate disrupted cell morphology

Table 4 Binding energy scores (kcal/mol) of the compounds identified in MF2d

Compounds	2BG1	6O93	1ZI0	1S14	1AI9	1AD1	4HDG	3QF4
Methoxyamine	−2.38	−2.10	−2.00	−2.15	−1.92	−2.20	−2.10	−1.93
Eudesmic acid	−4.79	−4.30	−4.60	−4.97	−5.32	−5.50	−6.20	−2.83
10-methyl anthracene-9-carboxaldehyde	−1.23	−6.00	−5.80	−4.20	−4.78	−5.50	−7.50	−3.89
Methyl-lathodoratin	−3.46	−5.00	−6.00	−4.93	−4.90	−6.20	−6.80	−4.30
2-Isopropyl-10-methyl phenanthrene	−4.22	−6.90	−6.50	−4.38	−4.89	−6.10	−8.40	−2.63

The full name of each protein, represented by the PDB ID herein, is given in Table 1

Staphylococcus epidermidis were susceptible, while all the Gram-negative bacteria tested were resistant. In contrast, Thielmann et al. (2019) reported the antibacterial activity of *M. cajuputi* essential oil against *S. aureus* DSM 1104 and *E. coli* DSM 1103, with MIC values ranging from 0.8 to 6.4 mg/mL. The MIC values obtained in this study are relatively low compared to the previous findings. This could be due to the purification process, as purifying plant extracts can concentrate bioactive compounds, enhancing their potency and effectiveness (Mani et al. 2022). The findings of this study are significant as the bacterial strains used in this study are commonly isolated from nosocomial infections and are
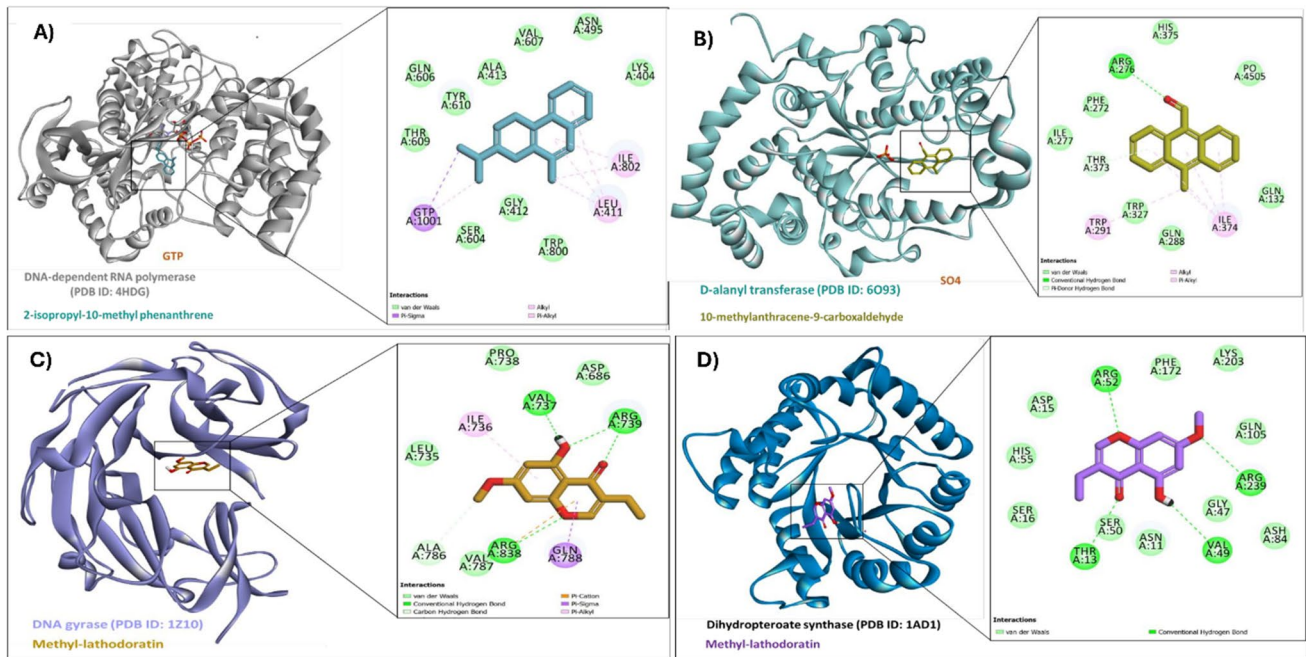
Fig. 6 **a)** Interaction between DNA-dependent DNA polymerase and 2-isopropyl-10-methyl phenanthrene **b)** D-alanyl transferase and 10-methyl anthracene-9-carboxaldehyde, **c)** DNA gyrase and methyl-lathodoratin, and **d)** dihydropteroate synthase and methyl-lathodoratin

primarily related to urinary tract infections (UTIs), pneumonia, invasive neonatal infections, and septicemia.

The FTIR analysis of MF2d revealed the presence of several valuable functional groups, including hydrocarbons, amines, aromatics, alcohols, phenol, ethers, and aryl groups. These results corroborate the findings by Paosen et al. (2017), who reported the presence of aromatic alkene, amine, alkanes, alcohols, ethers, esters, and carboxylic acid from the FTIR analysis of plants of the Myrtaceae family, including *M. cajuputi*. Meanwhile, the GC–MS analysis of MF2d identified 2-isopropyl-10-methyl phenanthrene, 10-methyl anthracene-9 carboxaldehyde, trimethyl gallic acid, methoxyamine, and methyl-lathodoratin. These results are consistent with previous reports by Hassan et al. (2022) and Mohamad Khairul Sahimi et al. (2022), who identified similar compounds in the GC–MS analysis of *M. cajuputi* extracts. These bioactive compounds may work together (synergy) or individually to provide a range of biological activities. For instance, 10-methyl anthracene-9-carboxaldehyde molecules with anthracene backbone may exist as anthraquinones with phenolic OH, interfering with any polyphenol-like proteins and resulting in microbial cell inactivation (Wink 2015). Furthermore, trimethyl gallic acid (phenolic) and methyl-lathodoratin (flavonoid) compounds were reported to form complexes that inactivate cellular proteins and microbial adhesins, ultimately killing the bacteria (Mohamad Khairul Sahimi et al. 2022).

The time-kill assay is a laboratory method used to evaluate the rate at which bacteria are killed and to understand how antimicrobial agents work. Additionally, it is used to ascertain the speed at which the concentration of an antimicrobial agent kills or inhibits bacteria under specific conditions (Adusei et al. 2019; Mogana et al. 2020). From the results of the time-kill assay, the bactericidal effect was first observed at 2 × MIC of MF2d after 8 and 12 h against S. *aureus* and *K. pneumoniae*, respectively. The time-kill responses of MF2d against S. *aureus* and *K. pneumoniae* showed concentration-dependent bactericidal effects.

Cell shrinkage, deep craters, and abnormal cell elongation were observed in the SEM images of MF2d-treated bacteria. This strongly suggests that the bioactive components in MF2d interfere with cell wall formation and membrane integrity. The effect could be due to the lead compound 2-isopropyl-10-methyl phenanthrene or the synergistic effect of all the compounds in MF2d. For example, the antibacterial action of phenanthrene derivatives has been linked to membrane rupture, which results in bacterial lysis due to internal osmotic pressure (Li et al. 2022). Similarly, it has been reported that anthracene derivatives such as 10-methyl anthracene-9-carboxaldehyde can interfere with protein synthesis, resulting in potential cellular damage (Wink 2015). Furthermore, methyl-lathodoratin is a flavonoid compound known for its ability to form complexes that neutralize cellular proteins and induce cell lysis (Mohamad Khairul Sahimi et al. 2022). Based on the SEM results, it is not possible to determine the exact target(s) of the active components on bacterial cells. However, the observed morphological changes strongly indicate that these bioactive compounds

disrupted cell wall function and cellular membrane integrity. In line with our findings, Cajuput candy has been shown to inhibit biofilm formation and alter the morphology of *C. albicans* and *S. mutans* (Septiana et al. 2019). Furthermore, *M. cajuputi* is rich in terpene and terpenoid compounds, reported to cause cellular damage and interfere with the cellular membrane function in *S. aureus* (Guimarães et al. 2019).

All eight (8) target bacterial proteins used in this study were docked with the five compounds identified in MF2d for molecular docking analysis to analyze the ligand–protein interactions. Antimicrobial agents are classified according to their mechanism of action, with the main classes being inhibitors of cell wall synthesis, protein synthesis, cell membrane function, nucleic acid synthesis, and antimetabolites (Alves et al. 2014). From the docked ligands, 2-isopropyl-10-methyl phenanthrene showed strong binding affinity (− 8.4 kcal/mol) toward DNA-dependent RNA polymerase, implying that the molecule may interfere with mRNA synthesis and DNA replication in bacteria (Alves et al. 2014). Likewise, 10-methylanthracene-9-carboxaldehyde showed moderate binding affinity to D-alanyl transferase with a docking score of − 6 kcal/mol. These enzymes are essential for bacterial cell wall shape and rigidity (Egan et al. 2020). As such, any antibacterial agent that interferes with cell wall rigidity may cause cell lysis due to internal osmotic pressure (Lima et al. 2020). Methyl-lathodoratin (flavonoid) showed moderate binding affinity towards dihydropteroate synthase (DHPS) and DNA gyrase, with respective binding energies of − 6.2 and − 6.0 kcal/mol. It is important to note that DHP synthase plays a significant role in folate metabolism in bacteria (Saqallah et al. 2022). Once the ligand–protein binding interaction is initiated, the ligand may inhibit the activity of DHP Synthase, thereby interfering with bacterial folate synthesis and causing the eventual death of bacteria. Similarly, DNA gyrase regulates DNA topology within bacterial cells (Dighe and Collet 2020). Consequently, binding a ligand to DNA gyrase may disrupt DNA synthesis, ultimately resulting in cellular damage. The findings of this study are consistent with previous reports that revealed flavonoid (kaempferol) as a potential candidate for antimicrobial agents with a strong binding affinity of − 8..0 kcal/mol towards DHP Synthase (Mir et al. 2022). Equally, Saqallah et al. (2022) reported moderate to strong binding affinities of phenolic and flavonoid compounds towards bacterial DHP Synthase and DNA gyrase B subunit with binding energies ranging between − 3.07 and − 10.05 kcal/mol. In another study, Ciprofloxacin, a standard antibacterial drug and known DNA gyrase inhibitor, has been observed to exhibit a binding energy of − 7.0 kcal/mol towards DNA gyrase (Yuan and Hao 2023). 2-isopropyl-10-methyl phenanthrene in this study scored docking energy (− 6.50 kcal/mol) comparable to Ciprofloxacin. Similarly, an inhibitor of DHP Synthase,

6-hydroxymethylpterin-diphosphate, has been observed to have a binding energy score of − 7.6 kcal/mol (Saqallah et al. 2022). However, methyl-lathodoratin (− 6.20 kcal/mol) showed less binding affinity to DHP Synthase than the standard inhibitor. The molecular docking results showed a significant binding propensity of the ligands identified in MF2d towards the target bacterial enzymes used in this study, demonstrating the potential of *M. cajuputi* as a novel source of antibacterial agents.

Conclusion

In conclusion, the findings of this study demonstrated that the MF2d sub-fraction from the methanolic extract of *M. cajuputi* leaf exhibited a strong antibacterial activity at relatively low MIC values. The antibacterial activity could be attributed to the major compound, 2-isopropyl-10-methyl phenanthrene, or the synergistic effects of all the active components, as indicated by their binding potential to the target bacterial proteins. Thus, these compounds can be lead candidates for developing antibacterial drugs targeting bacterial infections. The findings of this study could support the utilization of *M. cajuputi* as a novel source of therapeutic agents.

Declarations

Ethical statement No human or animal subjects were involved in this study.

Conflict of interest Musa Isah has no conflict of interest. Wan Abdul Wahab Wan-Nor-Amilah has no conflict of interest. Hasmah Abdullah has no conflict of interest. Shajarahtunnur Jamil has no conflict of interest. Mohd Dasuki Sul'ain has no conflict of interest. Abdullahi Ibrahim Uba has no conflict of interest. Gokhan Zengin has no conflict of interest. Dibyajit Lahiri has no conflict of interest. Hisham Atan Edinur has no conflict of interest. Wan Rosli Wan Ishak has no conflict of interest.

References

Abushaheen MA, Muzaheed FAJ, Alosaimi M, Mansy W, George M, Acharya S, Rathod S, Divakar DD, Jhugroo C, Vellappally S, Khan AA, Shaik J, Jhugroo P (2020) Antimicrobial resistance, mechanisms and its clinical significance. Dis Mon 66:100971. https://doi.org/10.1016/j.disamonth.2020.100971

Adusei EBA, Adosraku RK, Oppong-Kyekyeku J, Amengor CDK, Jibira Y (2019) Resistance modulation action, time-kill kinetics assay, and inhibition of biofilm formation effects of Plumbagin from *Plumbago zeylanica* Linn. J Trop Med 2019:1–8

Al-Abd NM, Mohamed Nor Z, Mansor M, Azhar F, Hasan MS, Kassim M (2015) Antioxidant, antibacterial activity, and phytochemical characterization of *Melaleuca cajuputi* extract. BMC Complement Altern Med 15:385. https://doi.org/10.1186/s12906-015-0914-y

Alves MJ, Froufe HJC, Costa AFT, Santos AF, Oliveira LG, Osório SRM, Abreu RMV, Pintado M, Ferreira ICFR (2014) Docking studies in target proteins involved in antibacterial action mechanisms: extending the knowledge on standard antibiotics to antimicrobial mushroom compounds. Molecules 19:1672–1684. https://doi.org/10.3390/molecules19021672

Anza M, Endale M, Cardona L, Cortes D, Eswaramoorthy R, Zueco J, Rico H, Trelis M, Abarca B (2021) Antimicrobial activity, in silico molecular docking, ADMET and DFT analysis of secondary metabolites from roots of three Ethiopian medicinal plants. Adv Appl Bioinform Chem 14:117–132. https://doi.org/10.2147/AABC.S323657

Awam UK (2023) *Melaleuca cajuputi* powell essential oil: a review of botanical, phytochemical and pharmacological properties. Borneo J Resour Sci Technol 13(2):1–12. https://doi.org/10.33736/bjrst.5314.2023

Bua A, Molicotti P, Donadu MG, Usai D, Le LS, Tran TTT, Ngo VQT, Marchetti M, Usai M, Cappuccinelli P, Zanetti S (2020) "In vitro" activity of *Melaleuca cajuputi* against mycobacterial species. Nat Prod Res 34(10):1494–1497. https://doi.org/10.1080/14786419.2018.150933

Chen BC, Lin CX, Chen NP, Gao CX, Zhao YJ, Qian CD (2018) Phenanthrene antibiotic targets bacterial membranes and kills *Staphylococcus aureus* with a low propensity for resistance development. Front Microbiol 9:1593. https://doi.org/10.3389/fmicb.2018.01593

Dighe SN, Collet TA (2020) Recent advances in DNA gyrase-targeted antimicrobial agents. Eur J Med Chem 199:112326. https://doi.org/10.1016/j.ejmech.2020.112326

Egan AJF, Errington J, Vollmer W (2020) Regulation of peptidoglycan synthesis and remodelling. Nat Rev Microbiol 18:446–460. https://doi.org/10.1038/s41579-020-0366-3

Erhabor RC, Aderogba MA, Erhabor JO, Nkadimeng SM, McGaw LJ (2021) In vitro bioactivity of the fractions and isolated compound from *Combretum elaeagnoides* leaf extract against selected food-borne pathogens. J Ethnopharmacol 273:113981. https://doi.org/10.1016/j.jep.2021.11398

Gorlenko CL, Kiselev HY, Budanova EV, Zamyatnin AA, Ikryannikova LN (2020) Plant secondary metabolites in the battle of drugs and drug-resistant bacteria: New heroes or worse clones of antibiotics? Antibiotics 9:170. https://doi.org/10.3390/antibiotics9040170

Guimarães AC, Meireles LM, Lemos MF, Cesar M, Guimarães C, Coutinho Endringer D, Fronza M, Scherer R (2019) Antibacterial activity of terpenes and terpenoids present in essential oils. Molecules 24:2471. https://doi.org/10.3390/molecules24132471

Hassan M, Abdalah A, Melad N, Zakariah MI, Asma N, Yusoff H, Hassan M, Abdalah A, Melad N, Zakariah MI, Asma N, Yusoff H, Life T (2022) Histopathological alterations in gills, liver and kidney of African catfish (*Clarias gariepinus,* Burchell 1822) exposed to *Melaleuca cajuputi* extract. Trop Life Sci Res 34:1–24

Isah M, Rosdi RA, Wan-Nor-Amilah WAW, Abdullah H, Sul'ain MD, Wan Ishak WW (2022) Phytoconstituents and biological activities of *Melaleuca cajuputi* powell: a scoping review. J Appl Pharm Sci 13(1):10–23. https://doi.org/10.7324/JAPS.2023.130102

Isnaini I, Biworo A, Khatimah H, Gufron KM, Puteri SR (2021) Antibacterial and antifungal activity of Galam (*Melaleuca cajuputi* subsp. Cumingiana (Turcz.) Barlow) extract against *E. coli* bacteria and *C. albicans* fungi. J Agromed Med Sci 7(2):79–83. https://doi.org/10.19184/ams.v7i2.23467

Khalaf MO, Abdel-Aziz MS, El-Hagrassi AM, Osman AF, Ghareeb MA, Khalaf OM, Abdel-Aziz MS, El-Hagrassi AM, Osman AF, Ghareeb MA (2021) Biochemical aspect, antimicrobial and antioxidant activities of *Melaleuca* and S*yzygium* Species (Myrtaceae) grown in Egypt. J Phys Conf Ser 1879:022062. https://doi.org/10.1088/1742-6596/1879/2/022062

Li J, Feng W, Dai R, Li B (2022) Recent progress on the identification of phenanthrene derivatives in traditional Chinese medicine and their biological activities. Pharmacol Res Mod Chin Med 3:100078. https://doi.org/10.1016/j.prmcm.2022.100078

Lima LM, Nascimento B, Barbosa G, Barreiro EJ (2020) Beta-lactam antibiotics: an overview from a medicinal chemistry perspective. Eur J Med Chem 208:112829. https://doi.org/10.1016/j.ejmech.2020.112829

Manandhar S, Luitel S, Dahal RK (2019) In vitro antimicrobial activity of some medicinal plants against human pathogenic bacteria. J Trop Med 2019:1895340. https://doi.org/10.1155/2019/1895340

Manga SS, Isah M, Kalgo M, Bazata AY (2017) Determination of antibacterial activity of aqueous extract of *Moringa oleifera* leaves against *Escherichia coli, Salmonella typhi* and *Pseudomonas aeruginosa*. Sch Bull 3:424–428

Mani J, Johnson J, Hosking H, Hoyos BE, Walsh KB, Neilsen P, Naiker M (2022) Bioassay-guided fractionation protocol for determining novel active compounds in selected Australian Flora. Plants 11:2886. https://doi.org/10.3390/plants11212886

Mera IFG, Falconí DEG, Córdova VM, Irina Francesca M, González FDEG, Córdova VM, Mera IFG, Falconí DEG, Córdova VM (2019) Secondary metabolites in plants: main classes, phytochemical analysis and pharmacological activities. Bionatura 4:1000–1009

Mir WR, Bhat BA, Rather MA, Muzamil S, Almilaibary A, Alkhanani M, Mir MA (2022) Molecular docking analysis and evaluation of the antimicrobial properties of the constituents of *Geranium wallichianum* D. Don ex Sweet from Kashmir Himalaya. Sci Rep 12:12547. https://doi.org/10.1038/s41598-022-16102-9

Mogana R, Adhikari A, Tzar MN, Ramliza R, Wiart C (2020) Antibacterial activities of the extracts, fractions and isolated compounds from *Canarium patentinervium* miq. against bacterial clinical isolates. BMC Complement Med Ther 20:55. https://doi.org/10.1186/s12906-020-2837-5

Mohamad Khairul Sahimi MB, Nagi AM, Hamdan NA, Zakariah MI, Yusoff NAH, Victor Tosin O, Hassan M (2022) Cajeput *Melaleuca cajuputi* extract supplementation in diets of *Macrobrachium rosenbergii*: Insight on the growth, immunological responses and resistance against Aeromonas hydrophila. Aquac Res 53:3441–3452. https://doi.org/10.1111/are.1585

Mroczek T, Dymek A, Widelski J, Wojtanowski KK (2020) The Bioassay-guided fractionation and identification of potent acetylcholinesterase inhibitors from *Narcissus* c.v' *Hawera*' using optimized vacuum liquid chromatography, high resolution mass spectrometry and bioautography. Metabolites 10:395. https://doi.org/10.3390/metabo10100395

My DTTA, Loan HTP, Hai NTT, Hieu DLT, Hoa PTT, Thuy DBTP, Quang PDT, Triet DNT, Van ADTT, Dieu DNTX, Trung DNT, Van HDN, Van TDP, Tung DVT, Nhung DNTA, My TTA, Loan HTP, Hai NTT, Hieu LT, Hoa TT, Thuy BTP, Quang DT, Triet NT, Van ATT, Dieu NTX, Trung NT, Van HN, Van TP, Tung VT, Nhung NTA (2020) Evaluation of the inhibitory activities of COVID-19 of *Melaleuca cajuputi* oil using docking simulation. ChemistrySelect 5:6312–6320. https://doi.org/10.1002/slct.202000822

Nandiyanto ABD, Oktiani R, Ragadhita R (2019) How to read and interpret FTIR spectroscope of organic material. Indones J Sci Technol 4(1):97–118. https://doi.org/10.17509/ijost.v4i1.15806

Paosen S, Saising J, Wira Septama A, Piyawan Voravuthikunchai S (2017) Green synthesis of silver nanoparticles using plants from Myrtaceae family and characterization of their antibacterial activity. Mater Lett 209:201–206. https://doi.org/10.1016/j.matlet.2017.07.102

Saqallah FG, Hamed WM, Talib WH, Dianita R, Wahab HA (2022) Antimicrobial activity and molecular docking screening of bioactive components of *Antirrhinum majus* (snapdragon) aerial parts. Heliyon 8:e10391. https://doi.org/10.1016/j.heliyon.2022.e10391

Septiana S, Bachtiar BM, Yuliana N, Wijaya CH (2019) Cajuputs candy impairs Candida albicans and S*treptococcus mutans* mixed biofilm formation in vitro. F1000Research 8:1–25

Septiana S, Yuliana ND, Bachtiar BM, Putri SP, Fukusaki E, Laviña WA, Wijaya CH (2020) Metabolomics approach for determining potential metabolites correlated with sensory attributes of *Melaleuca cajuputi* essential oil, a promising flavor ingredient. J Biosci Bioeng 129(5):581–587. https://doi.org/10.1016/j.jbiosc.2019.12.005

Shubham B, Verma R, Gupta J (2018) Challenges and future prospects of herbal medicine. Int Res Med Heal Sci 1(2):12–15

Thielmann J, Muranyi P, Kazman P (2019) Screening essential oils for their antimicrobial activities against the foodborne pathogenic bacteria *Escherichia coli* and *Staphylococcus aureus*. Heliyon 5:e01860. https://doi.org/10.1016/j.heliyon.2019.e01860

Toan TQ, Thao LPP, Chien NQ, Van NTH, Phuong ĐL, Huong TT, Quan PM, Inh CT, Minh PTH, Bich HT, Ngan TTK, van Thai T, Viet NT, Bach LG, Long PQ (2020) Determination of chemical composition and antimicrobial activity of *Melaleuca cajuputi* essential oil from Quang Tri Province, Vietnam. Asian J Chem 32:2203–2207

Wan-Nor-Amilah WAW, Jia-Hui L, Isah M, Sul'ain MD (2022) In vitro anti-Candida activity of *Melaleuca cajuputi* extract. Malays J Microbiol 18:612–619. https://doi.org/10.21161/mjm.221510

Wink M (2015) Modes of action of herbal medicines and plant secondary metabolites. Med 2:251–286. https://doi.org/10.3390/medicines2030251

Yuan C, Hao X (2023) Antibacterial mechanism of action and in silico molecular docking studies of *Cupressus funebris* essential oil against drug resistant bacterial strains. Heliyon 9(8):e18742. https://doi.org/10.1016/j.heliyon.2023.e18742

Zengin G, Dall'Acqua S, Sinan KI, Uba AI, Sut S, Peron G, Etienne OK, Kumar M, Cespedes-Acuña CL, Alarcon-Enos J, Mollica A, Mahomoodally MF (2022) Gathering scientific evidence for a new bioactive natural ingredient: the combination between chemical profiles and biological activities of *Flueggea virosa* extracts. Food Biosci 49:101967. https://doi.org/10.1016/j.fbio.2022.101967